ISSN 1674-1056
http://cpb.iphy.ac.cn
http://iopscience.iop.org/cpb
中国物理 B
Chinese Physics
中国物理
Chinese Physics B

Degradation of current-voltage and low frequency noise characteristics under negative bias illumination stress in InZnO thin film transistors

Li Wang(王黎), Yuan Liu(刘远), Kui-Wei Geng(耿魁伟), Ya-Yi Chen(陈雅怡), Yun-Fei En(恩云飞)
Citation: Chin. Phys. B . 2018, 27(6): 068504. **doi:** 10.1088/1674-1056/27/6/068504

Journal homepage: http://cpb.iphy.ac.cn; http://iopscience.iop.org/cpb

What follows is a list of articles you may be interested in

Technology demonstration of a novel poly-Si nanowire thin film transistor

Libin Liu(刘立滨), Renrong Liang(梁仁荣), Bolin Shan(单柏霖), Jun Xu(许军), Jing Wang(王敬)
Chin. Phys. B . 2016, 25(11): 118504. **doi:** 10.1088/1674-1056/25/11/118504

Improvement in the electrical performance and bias-stress stability of dual-active-layered silicon zinc oxide/zinc oxide thin-film transistor

Yu-Rong Liu(刘玉荣), Gao-Wei Zhao(赵高位), Pai-To Lai(黎沛涛), Ruo-He Yao(姚若河)
Chin. Phys. B . 2016, 25(8): 088503. **doi:** 10.1088/1674-1056/25/8/088503

Influence of white light illumination on the performance of a-IGZO thin film transistor under positive gate-bias stress

Tang Lan-Feng, Yu Guang, Lu Hai, Wu Chen-Fei, Qian Hui-Min, Zhou Dong, Zhang Rong, Zheng You-Dou, Huang Xiao-Ming
Chin. Phys. B . 2015, 24(8): 088504. **doi:** 10.1088/1674-1056/24/8/088504

A simple and accurate method to measure program/erase speed in a memory capacitor structure

Jin Lin, Zhang Man-Hong, Huo Zong-Liang, Wang Yong, Yu Zhao-An, Jiang Dan-Dan, Chen Jun-Ning, Liu Ming
Chin. Phys. B . 2013, 22(1): 018501. **doi:** 10.1088/1674-1056/22/1/018501

High-photosensitivity polymer thin-film transistors based on poly(3-hexylthiophene)

Liu Yu-Rong, Lai Pei-Tao, Yao Ruo-He
Chin. Phys. B . 2012, 21(8): 088503. **doi:** 10.1088/1674-1056/21/8/088503

Degradation of current–voltage and low frequency noise characteristics under negative bias illumination stress in InZnO thin film transistors*

Li Wang(王黎)[1,2,3], Yuan Liu(刘远)[1,2,3,†], Kui-Wei Geng(耿魁伟)[1], Ya-Yi Chen(陈雅怡)[1,2], and Yun-Fei En(恩云飞)[2]

[1] *School of Electronic and Information Engineering, South China University of Technology, Guangzhou* 510640, *China*
[2] *Science and Technology on Reliability Physics and Application of Electronic Component Laboratory, CEPREI, Guangzhou* 510610, *China*
[3] *Key Laboratory of Silicon Device Technology, Chinese Academy of Sciences, Beijing* 100029, *China*

(Received 12 December 2017; revised manuscript received 19 January 2018; published online 10 May 2018)

The instabilities of indium–zinc oxide thin film transistors under bias and/or illumination stress are studied in this paper. Firstly, illumination experiments are performed, which indicates the variations of current–voltage characteristics and electrical parameters (such as threshold voltage and sub-threshold swing) are dominated by the stress-induced ionized oxygen vacancies and acceptor-like states. The dependence of degradation on light wavelength is also investigated. More negative shift of threshold voltage and greater sub-threshold swing are observed with the decrease of light wavelength. Subsequently, a negative bias illumination stress experiment is carried out. The degradation of the device is aggravated due to the decrease of recombination effects between ionized oxygen vacancies and free carriers. Moreover, the contributions of ionized oxygen vacancies and acceptor-like states are separated by using the mid-gap method. In addition, ionized oxygen vacancies are partially recombined at room temperature and fully recombined at high temperature. Finally, low-frequency noise is measured before and after negative bias illumination stress. Experimental results show few variations of the oxide trapped charges are generated during stress, which is consistent with the proposed mechanism.

Keywords: indium–zinc oxide, thin film transistor, illumination, low frequency noise

PACS: 85.30.Tv, 73.40.Qv, 71.23.Cq, 73.50.Dn **DOI:** 10.1088/1674-1056/27/6/068504

1. Introduction

Due to its excellent electrical performance and good stability,[1] the amorphous indium zinc oxide thin film transistor (a-IZO TFT) is drawing a great deal of attention in the next generation of active matrix liquid crystal displays (AMLCD) and active matrix organic light emitting diodes (AMOLED).[2] During its application, the device may be exposed to variable environments, such as illumination, temperature, humidity, etc. As reported in Refs. [3]–[6], the electrical characteristics and the typical parameters of IZO TFTs may change in the above environments, which may further influence the performances of the image capture and display system. Moreover, IZO TFTs may be simultaneously subjected to diverse stresses. In particular, the degradation of the device under bias illumination stress may be more serious and thus it should be investigated before its application in the consumer market.

The instability of TFT under illumination and/or gate bias stress has been studied by many groups.[7–14] As reported, the notable degradations of current–voltage (I–V) and capacitance–voltage (C–V) characteristics have been studied under the above bias illumination stress.[12,13] These degeneration phenomena can be attributed to the formation of localized states and the fixed oxide trapped charges.[10,12] The formation of localized states mainly arises from the generation of ionized oxygen vacancies in the channel while the formation of oxide trapped charges is due to the occupation of neutral traps in the gate oxide.[13,14] However, few papers have reported the low frequency noise (LFN) characteristics of IZO TFTs after negative bias illumination stress (NBIS). The low frequency noise of the devices may limit the minimum signal level that can be correctly detected by the subsequent circuit. Moreover, the low frequency noise may be up-converted into phase noise and high frequency noise in some conditions, which may affect the linearly of an analog circuit.[15] Thus, the noise performance of IZO TFT needs to be analyzed and minimized.

Flicker ($1/f$) noise is a random fluctuation phenomenon in a semiconductor device and it is sensitive to semiconductor quality and device defects. As a non-destructive reliability characterization method, $1/f$ noise measurement has been widely used in the evaluation and selection of BJT, MOS, GaN, semiconductor lasers, and other devices.[16] In addition, the energy and spatial distribution of traps can be extracted and the degeneracy of the devices can be analyzed by $1/f$ noise.

In this paper, a series of experiments is performed to study the stabilities of IZO TFTs under illumination and/or electrical

*Project supported by the Opening Fund of Key Laboratory of Silicon Device Technology, Chinese Academy of Sciences (Grant No. KLSDTJJ2018-6), the National Natural Science Foundation of China (Grant No. 61574048), the Science and Technology Research Project of Guangdong Province, China (Grant No. 2015B090912002), and the Pearl River S & T Nova Program of Guangzhou City, China (Grant No. 201710010172).

†Corresponding author. E-mail: Liuyuan@ceprei.com

© 2018 Chinese Physical Society and IOP Publishing Ltd

stress. The dependence of degradation characteristics on the illumination wavelength is also analyzed. The contributions of stresses induced ionized oxide vacancies (V_o^{2+}) and acceptor-like states are separated. Furthermore, the LFN is measured before and after NBIS. The concentrations of traps near the IZO/SiO_2 interface are extracted and the spatial distributions of trapped charges in the gate oxide are calculated.

2. Device performance and low frequency noise measurement

2.1. Devices structure and *I–V* characteristics

The device under test is IZO TFT with bottom gate structure as shown in Fig. 1. A 300-nm-thick layer of aluminum gate was sputtered and patterned by wet etching. Then, the insulating layer, including 50 nm of SiO_2 and 250 nm of SiN_x, was deposited by plasma-enhanced chemical vapor deposition (PECVD) at 310 °C. Subsequently, an IZO layer of 30 nm was deposited by radio frequency magnetron sputtering. A stacked structure of molybdenum/aluminum/molybdenum (25 nm /100 nm /25 nm), used as source and drain electrodes, was formed via sputtering and patterned by lift-off technology, which controls the channel length and width. Finally, the device was passivized by a 300-nm-thick SiO_2 layer grown by PECVD.[17] In experiment, all devices had the same channel width/length i.e., 20 μm/10 μm, specifically. The measured unit area gate oxide capacitance (C_{ox}) was about 14.1 nF.

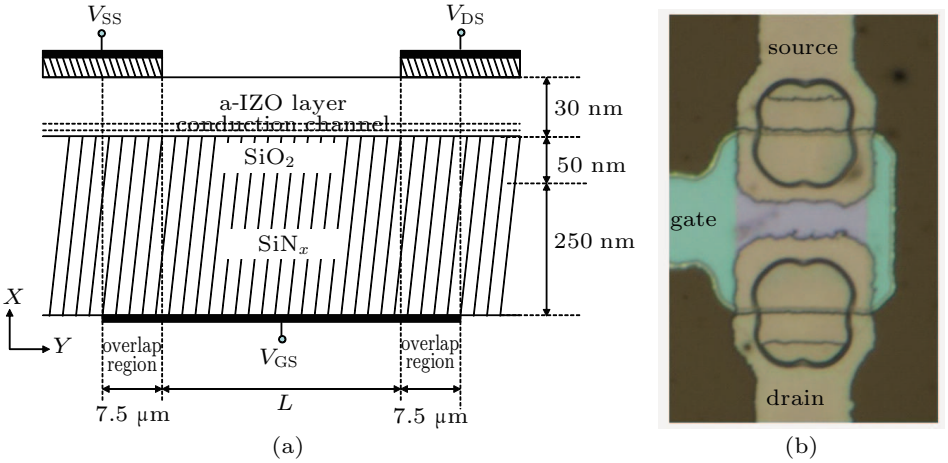


Fig. 1. (color online) (a) Cross-sectional view and (b) micrograph of IZO TFT.

The transfer characteristics of the device are shown in Fig. 2. The calculated threshold voltage (V_{th}) is about 4.35 V, the field effect mobility (μ_{FE}) is about 25.62 $cm^2 \cdot V^{-1} \cdot s^{-1}$, and sub-threshold swing (SS) is about 0.4 V/dec. It was reported in Refs. [18] and [19] that the oxygen vacancies (V_o) act as the dominant native point defects in metal oxide. The transition level from +2 to 0 is close to the conduction band minimum (CBM), the ionized V_o is a shallow donor and thus gives rise to the n-type conductivity in metal oxide.

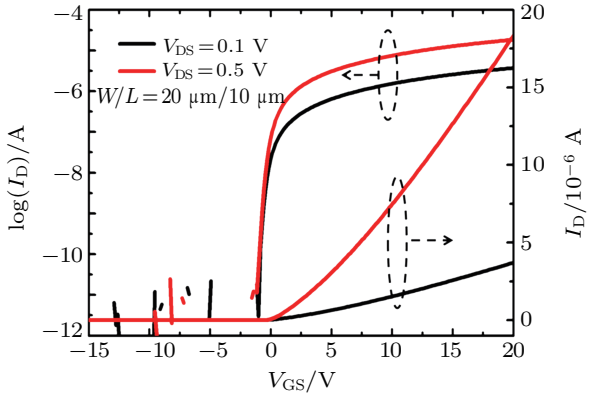


Fig. 2. (color online) Transfer characteristics in the IZO TFT under different values of V_{DS}.

Good stability of IZO TFT is shown in this experiment. The measured transfer curves of the device under NBS stress with $V_{GS} = -10$ V are plotted in Fig. 3. Indistinguishable variations of transfer characteristics are observed with the increase of stress time. In oxide thin film transistors, the density of deep states in the bottom half of the band-gap is approximately 5×10^{20} cm^{-3}.[20] Therefore, the Fermi level is pinned at deep levels and few holes may accumulate in the channel with a negative voltage. Thus, a small fraction of accumulated holes may inject into the gate oxide and less variation of V_{th} can be observed.

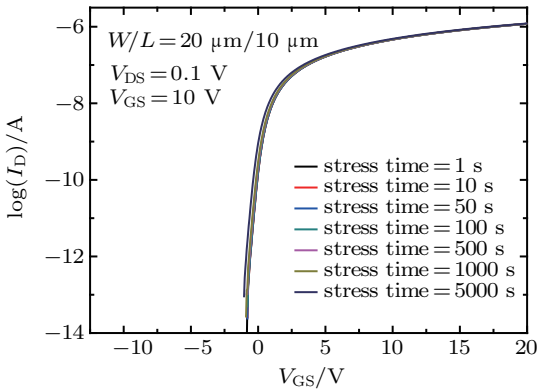


Fig. 3. (color online) Variations of transfer curves under different negative bias stresses ($V_{GS} = -10$ V).

2.2. Low frequency noise measurement

The measurement setup of drain current noise power spectra of IZO TFTs is illustrated in Fig. 4.[21] The electrical properties of IZO TFTs were measured by an Agilent B1500. The ADQ214 was used to measure the noise power spectral density of the device. The Keysight E4727A was adopted to construct the filter and amplifier units of the noise test system. The matching resistance R_G and R_D were selected by waferpro based on the bias condition.

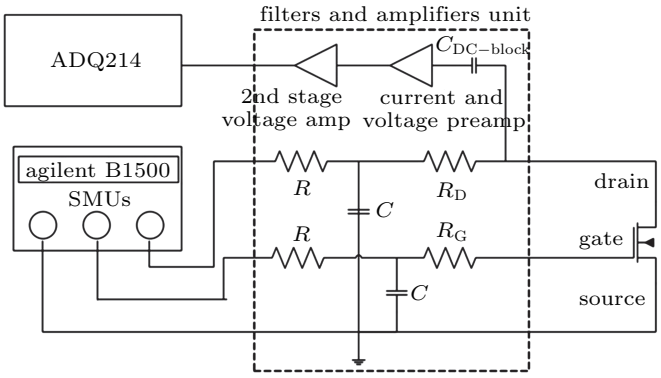


Fig. 4. Measurement setup of low frequency noise in IZO TFT.

3. Illumination induced degradation in IZO TFT

In this section, a series of illumination experiments were performed. The degradations of IZO TFTs under monochromatic illumination were studied. The dependence of degradation characteristic on wavelength was then analyzed. In this experiment, the used light intensity was 5 mW/cm^2 and wavelengths were 635 nm, 515 nm, 450 nm, and 405 nm.

Transfer characteristics of IZO TFTs exposed to blue laser light ($\lambda = 450$ nm) are shown in Fig. 5. The photon energy of blue light in this experiment was about 2.8 eV calculated by the Planck equation:

$$e = hv = \frac{hc}{\lambda}, \tag{1}$$

h is the Planck constant, and its value is 4.14×10^{-15} eV; c is the speed of light in a vacuum; λ is the wavelength that corresponds to the light energy. As shown in Fig. 5, a parallel negative shift of the transfer characteristic after illumination (curve b) is found compared with that before illumination (curve a). The calculated V_{th} varies from 4.34 V to 3.15 V while few variations of sub-threshold swing are observed. Furthermore, larger sub-threshold current and sub-threshold swing are observed under illumination (curve c) than that measured in the dark (curve b).

As reported in Ref. [22], donor-like states and acceptor-like states may exist in the channel. The donor-like states are neutral because the occupied electrons and positive are neutralized while being emptied. The negative shift of I–V characteristic curve after illumination may relate to donor-like states (oxygen vacancies, V_o.[13] As reported in Refs. [23]–[25], a large number of V_o exist on the top of the valence band. The Fermi level in the IZO/SiO_2 interface lowers nearly to midgap in a case with applying negative gate voltage. Therefore, oxygen vacancies can be photo-excited and becomeV_o^{2+}. These V_o^{2+} become stable due to outward relaxations of neighboring metal atoms after long time illumination. Therefore, the generated deep-level V_o^{2+} may act as positive fixed charges existing near the IZO/SiO_2 interface, which effectively screen the gate bias and then result in related negative shifts of I–V curves as shown in Fig. 5. However, there are also the latest reports[18,19] indicating that the oxygen vacancies exist near the conduction band minimum rather than what the traditional opinion says, specifically oxygen vacancies are at a deep level. The V_o is +2 charged near the CBM, which may influence the IZO TFT stability under stress (especially temperature). The stability of the device is affected by the decrease of the oxygen vacancy defects, which are located near CBM when annealed at above the crystallization temperature.

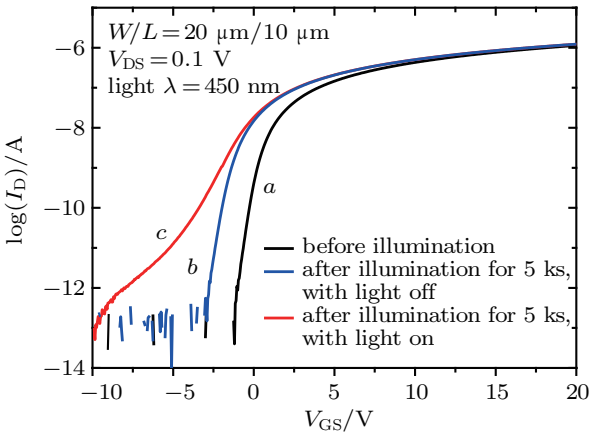


Fig. 5. (color online) Plots of I–V characteristic curves of IZO TFTs under blue illumination.

The notable sub-threshold currents observed under illumination are due to the optically generated free carriers. As shown in Fig. 6, the optically generated carriers may relate to three main mechanisms during light exposure. (i) Electrons are directly excited from the valence band to the conduction band. (ii) Electrons in deep level traps of band-gap are excited to the conduction band, which is accompanied by the generation of sub-gap states. (iii) Holes in traps above Fermi level of the band gap are excited to the valence band with defects generated at the same time. In this experiment, the photon energy of blue light is less than the band gap of a-IZO layer and mechanism (i) may not happen. In addition, the density of holes in the upper half of the band gap is very low and mechanism (iii) may not dominate. Therefore, the optically generated carriers may dominate by mechanism (ii), which relates to free electrons excited from V_o and acceptor-like states below the Fermi level. As reported in Ref. [24], the sub-threshold swing only

relates to the density of acceptor-like deep states. As shown in Fig. 5, the sub-threshold swing becomes larger during illumination and quickly recovers in the dark. This phenomenon indicates that the excess sub-threshold current may dominate by the excitation process of electrons from acceptor-like states below the Fermi level.

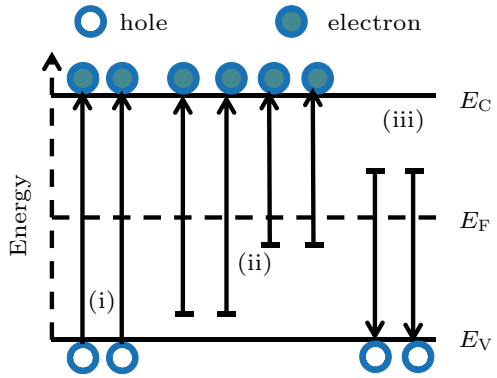


Fig. 6. (color online) Generating mechanism of free carriers under blue illumination.

The plots of $\log(I_D)$ versus V_{GS} in the IZO TFTs with the illumination of four different wavelengths are shown in Fig. 7. Like the above discussion, the sub-threshold current increases with the decrease of wavelength, which is also caused by photo-generated electrons released by acceptor-like deep states and donor-like states under illumination. As shown in the inset of Fig. 7, more negative shifts of V_{th} are observed in the range of wavelength from 625 nm to 405 nm. This phenomenon indicates that V_o^{2+} may be generated by photon excitation with the photon energy increasing.

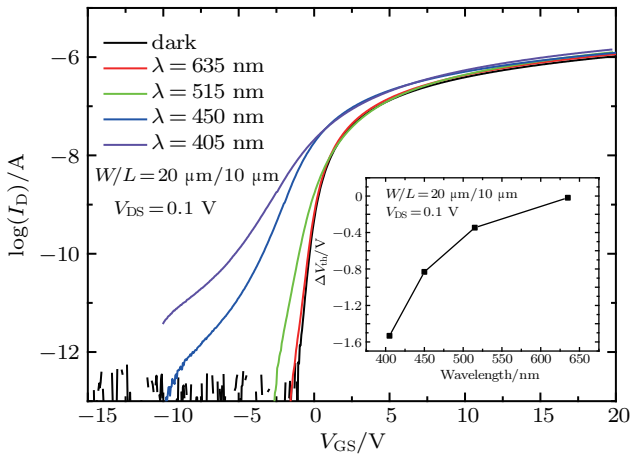


Fig. 7. (color online) Transfer characteristics under long time illumination (5000 s) with four wavelengths.

4. Instabilities under negative bias illumination stress

4.1. Degradation of *I–V* characteristics

Figure 8 shows the measured transfer characteristics of IZO TFTs during NBIS when V_{GS} is about −10 V and the light wavelength is about 450 nm.[26,27] The energy of the selected wavelength needs to be greater than the ionization energy of oxygen vacancy and smaller than the band gap of IZO. The value of ΔV_{th} after stress is about −3.15 V, which is more serious than that measured under the illumination stress. The sub-threshold swing is also varied from 0.4 V/dec to 1.7 V/dec, which may be due to the change of acceptor-like states. As reported in Ref. [28], the degradation induced by NBIS can also be explained by the oxygen vacancy model, which is shown in Fig. 9. The electrons are swept from the IZO/SiO_2 interface to the back IZO/passivation interface under an applied negative gate voltage. In addition, V_o^{2+} can also be moved and accumulated in the IZO/SiO_2 interface.[13,29] Since the electrons in the IZO/SiO_2 interface are depleted, the recombination effect between V_o^{2+} and electrons strongly decrease during stress. Thus, more V_o^{2+} are formed, and greater degradation of V_{th} is observed.

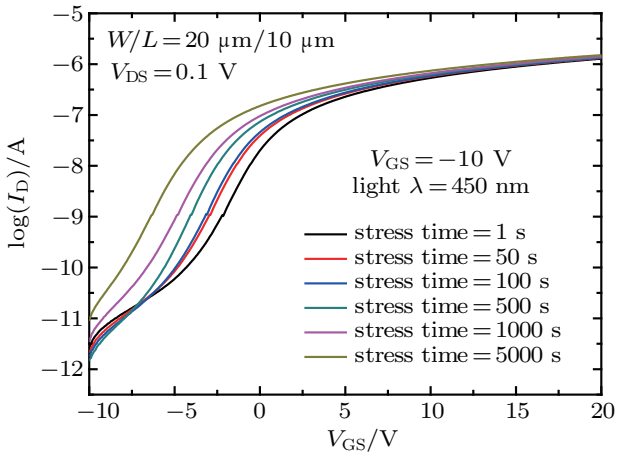


Fig. 8. (color online) Transfer curves of IZO TFT, measured under different illumination stress times.

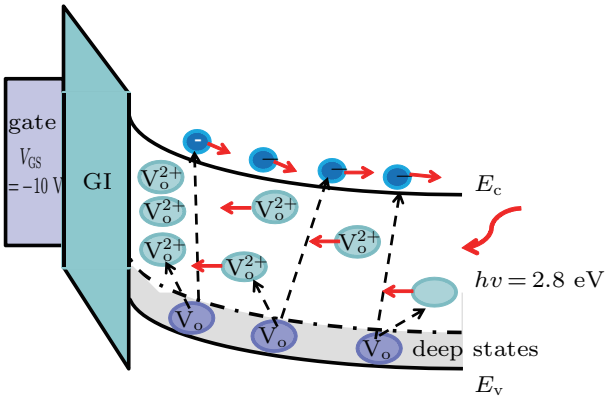


Fig. 9. (color online) Oxygen vacancy model under NBIS.

The variation of the threshold voltage during stress may simultaneously be affected by photo-generated ionized oxygen vacancies (with surface density $Q_{ov} = q\Delta N_{ov}$) and the generation of acceptor-like deep states in the IZO/SiO_2 inter-

face (with surface density $Q_{\rm deep} = q\Delta N_{\rm deep}$), and it can be expressed as[30]

$$\Delta V_{\rm th} = \Delta V_{\rm ov} + \Delta V_{\rm deep} = -\frac{q\Delta N_{\rm ov}}{C_{\rm ox}} + \frac{q\Delta N_{\rm deep}}{C_{\rm ox}}. \quad (2)$$

The values of $\Delta V_{\rm ov}$ and $\Delta V_{\rm deep}$ can be extracted using the procedure proposed by McWhorter and Winokur,[31] the acceptor-like deep states are neutral at the midgap, and only the oxygen vacancies can affect the shift of midgap voltage as given as

$$\Delta V_{\rm MG} = -\frac{q\Delta N_{\rm ov}}{C_{\rm ox}}. \quad (3)$$

The $V_{\rm MG}$ is the gate voltage at which the sub-threshold current flows under the midgap condition. Since the device is of an amorphous semiconductor, the sub-threshold current in the $V_{\rm MG}$ can be expressed as[31]

$$I_{\rm D} = \mu_{\rm n}\frac{W}{L}KT\sqrt{\frac{\varepsilon_0\varepsilon_{\rm s}}{2qn_{\rm i}}\frac{KT}{q}}n_{\rm i}\left[1-\exp\left(-\frac{qV_{\rm D}}{KT}\right)\right] \times \exp\left(\frac{q\varphi_{\rm s}}{KT}\right). \quad (4)$$

Here, $\mu_{\rm n}$ is the electron mobility at room temperature, ε_0 is the vacuum dielectric constant, $n_{\rm i}$ is the carrier concentration at room temperature, and the value of $\varphi_{\rm s}$ at the midgap is 0. The value of sub-threshold current, calculated in $V_{\rm MG}$ is about 3.88×10^{-10} A, which can be used to extract the value of $\Delta V_{\rm MG}$. Then, the number of oxygen vacancies can also be extracted by using the midgap voltage. According to Eq. (2), $\Delta N_{\rm deep}$ can be extracted from the experimental threshold voltage ($\Delta V_{\rm th}$) and the calculated number of oxygen vacancies ($\Delta V_{\rm ov}$).

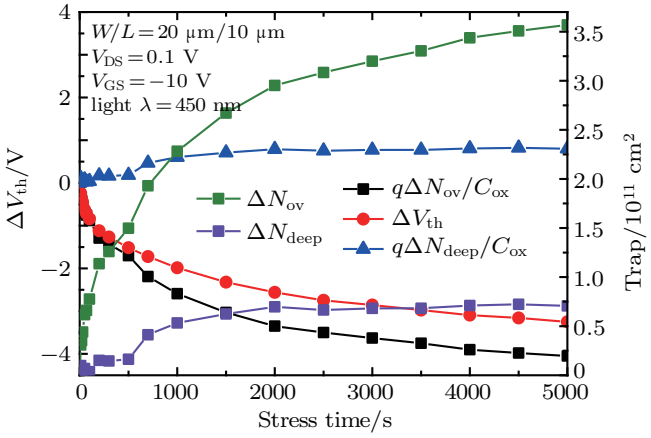


Fig. 10. (color online) Separations of stress induced ionized oxygen vacancies and acceptor-like states.

The extracted variations of oxygen vacancies and acceptor-like states in the channel layer are plotted in Fig. 10. It is obviously shown that the shift of threshold voltage is dominated by ionized oxygen vacancies, which causes the negative shift of $V_{\rm th}$. Since the electrons at the interface are depleted, more $V_{\rm o}^{2+}$ may accumulate near the interface and be fixed. In addition, the generation of acceptor-like states not only causes the threshold voltage to shift toward positive but also increases the sub-threshold swing as shown in Fig. 10.

4.2. Annealing characteristic after negative bias illumination stress

The annealing characteristics of IZO TFTs after NBIS are graphed in Fig. 11. The extracted values of $\Delta V_{\rm th}$ in stress and annealing process are shown in Fig. 12. In the annealing process, the two-phase annealing phenomenon is present. An instant recovery may happen at the end of the stress, and then recovery of the device tends to be saturated. As described above, the variation of $V_{\rm th}$ is mainly caused by the ionized oxygen vacancies. Therefore, the phenomenon indicates that the partially unstable $V_{\rm o}^{2+}$ are recombined with the electrons immediately at the end of the stress and the relatively stable $V_{\rm o}^{2+}$ can keep fixed at the IZO/SiO_2 interface. As shown in Fig. 11, the device does not recover to the initial states after 20 h at room temperature. The stable $V_{\rm o}^{2+}$ may be formed due to the outward relaxation and metal atoms moving to positions far away from their initial positions. The above stable $V_{\rm o}^{2+}$ cannot be easily recovered at room temperature. However, the device characteristics can fully resume to the initial state and the crystal structure is not changed by annealing in the air (The annealing atmospheres have no effect on the device stability due to the 300-nm passivation layer on the surface of the device.[32]) for 10 h at 120 °C, which indicates that those stable $V_{\rm o}^{2+}$ can be recovered after obtaining enough external energy.

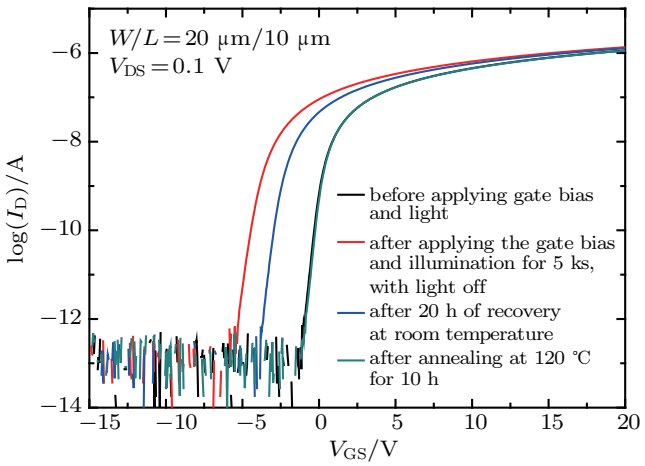


Fig. 11. (color online) Annealing characteristics under different NBIS conditions.

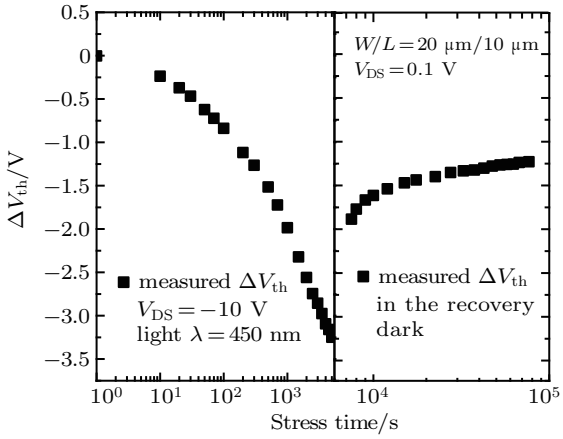


Fig. 12. Extracted $\Delta V_{\rm th}$ versus stress time in stress and annealing process.

4.3. LFN characteristics before and after NBIS

The curves of measured normalized drain current power spectral densities versus drain current before and after stress are shown in Fig. 13. According to the carrier number fluctuation model, the normalized current spectral density of IZO TFTs can be expressed as[33]

$$S_{\rm ID}/I_{\rm D}^2 = \left(\frac{g_{\rm m}}{I_{\rm D}}\right)^2 S_{V_{\rm fb}} = \left(\frac{g_{\rm m}}{I_{\rm D}}\right)^2 \left(\frac{q^2 KT\lambda N_{\rm t}}{WC_{\rm ox}^2 f}\right), \quad (5)$$

where $g_{\rm m}$ is the device transconductance, $S_{V_{\rm fb}}$ is the flat-band voltage spectral density, $N_{\rm t}$ is the trap concentration, and λ is the tunneling attenuation coefficient, which is about 0.1 nm for SiO_2.[34]

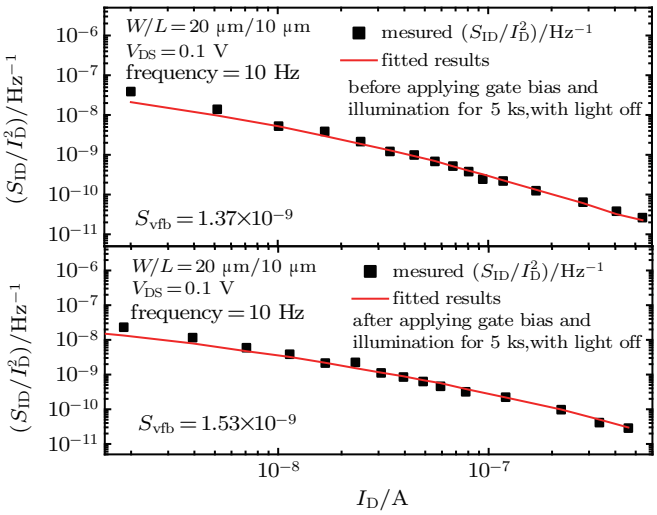


Fig. 13. (color online) Curves of normalized noise versus drain current power spectral density after NBIS.

Based on Fig. 13, the flat-band voltage spectral densities can be extracted to be about 1.37×10^9 $V^2 \cdot Hz^{-1}$ and 1.53×10^9 $V^2 \cdot Hz^{-1}$, respectively. According to Eq. (5), the extracted N_t values are about 8.18×10^{17} $cm^{-3} \cdot eV^{-1}$ before NBIS and about 9.14×10^{17} $cm^{-3} \cdot eV^{-1}$ after NBIS, respectively. As reported in Ref. [35], the noise spectrum originated from carriers exchanging between the channel and traps in the gate dielectric. The low frequency noise further reveals that the total of localized states and trapped charges in the gate insulator increases after NIBS.

In order to have a qualitative spatial distribution of trapped charges in the gate oxide, the frequency is converted into the tunneling depth as follows:[36–39]

$$\frac{1}{2\pi f} = \tau_0 \exp(\alpha_{\rm t} x), \quad (6)$$

where τ_0 is the time constant at the IZO/SiO_2 interface, x is the distance from the interface to the gate oxide, $\alpha_{\rm t}$ is the tunneling attenuation coefficient, which is about 10^8 cm^{-1} for SiO_2. The value of τ_0 is equal to 10^{-10} s for traps distributed near the interface. Equation (6) states that the probability of penetration into the gate oxide decreases exponentially with distance. The extracted density profiles of trapped charges before and after stress are shown in Fig. 14. Negligible shifts of defect space distribution curves before and after stress can be observed, which indicates that few trapped charges are formed during stress, which is consistent with the theory discussed in the above section. This phenomenon also verifies that the NBIS effect of IZO TFTs may be dominated by ionized oxygen vacancies at the IZO/SiO_2 interface.

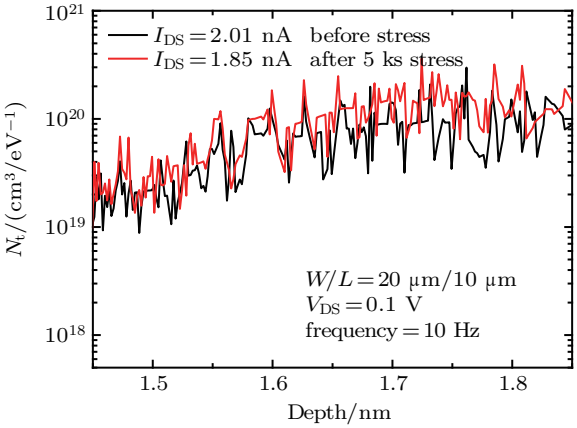


Fig. 14. (color online) Spatial distributions of oxide trapped charge density in gate oxide before and after stress.

5. Conclusions

Instability of IZO TFT under negative bias illumination stress has been discussed in this paper. The degradation effects of IZO TFT may be dominated by ionized oxygen vacancies. More negative shifts of threshold voltage under illumination can be observed with the decrease of light wavelength. Furthermore, electrons captured by acceptor-like states below Fermi-level may be photo-excited and thus lead to the increase of sub-threshold current and sub-threshold swing. In addition, LFN measurement is performed before and after negative bias

illumination stress separately. Indistinguishable variation in spatial distribution of oxide trapped charges is observed after stress, which is consistent with the proposed degradation mechanism.

References

[1] Lan L, Xiong N, Xiao P, Li M, Xu H, Yao R and Wen Sand Peng J 2013 *Appl. Phys. Lett.* **102** 242102

[2] Fortunato E, Barquinha P and and Martins R 2012 *Adv. Mater.* **24** 2945

[3] Lee K H, Ji S J, Son K S and Park J S 2009 *Appl. Phys. Lett.* **95** 1309

[4] Tang L F, Lu H and Ren F 2016 *Chin. Phys. Lett.* **33** 038502

[5] Huang X, Wu C, Lu H and Ren F 2012 *Appl. Phys. Lett.* **100** 243505

[6] Chang G W, Chang T C, Jhu J C and Tsai T M 2014 *IEEE Electron. Dev. Lett.* **61** 2119

[7] Nomura K, Kamiya T, Hirano M and and Hosono H 2009 *Appl. Phys. Lett.* **95** 013502

[8] Chowdhury M D H, Migliorato P and and Jang J 2011 *Appl. Phys. Lett.* **98** 153511

[9] Chowdhury M D H, Ryu S H, Migliorato P and and Jang J 2011 *J. Appl. Phys.* **110** 114503

[10] Chen T C, Chang T C, Hsieh T Y, Tsai C T, Chen S C, Lin C S, Jian F Y and Tsai M Y 2011 *Thin Solid Films* **520** 1422

[11] Nomura K, Kamiya T and Hosono H 2011 *Appl. Phys. Lett.* **99** 488

[12] Gwang Um J, Mativenga M, Migliorato P and Jang J 2012 *Appl. Phys. Lett.* **101** 468

[13] Oh H, Yoon S, Ryu M K, Hwang C, Yang S and Park S K 2010 *Appl. Phys. Lett.* **97** 488

[14] Migliorato P, Md D H C, Gwang Um J and Seok M 2012 *Appl. Phys. Lett.* **101** 2945

[15] Tseng Y C, Huang W M, Spears E, Spooner D, Ngo D and Ford J M 2002 *IEEE Electron Dev. Lett.* **20** 54

[16] Fung T C, Baek G and Kanicki J 2010 *J. Appl. Phys.* **108** 074518

[17] Liu Y, Chen R S, Li B, En Y F and Chen Y Q 2018 *IEEE Trans. Electron. Dev.* **65** 356

[18] Kim H, Choi D, Park S, Park K, Park H W, Chung K B and Kwon J Y 2017 *Appl. Phys. Lett.* **110** 232104

[19] Liu L, Mei Z, Tang A, Azarov A, Kuznetsov K, Xue Q K and Du X 2016 *Phys. Rev. B* **93** 235305

[20] Nomura K, Kamiya T, Yanagi H, Ikenaga E, Yang K, Kobayashi K, Hirano M and Hosono H 2008 *Appl. Phys. Lett.* **92** 202117

[21] Fung T C, Back G and Kanicki 2010 *J. Appl. Phys.* **108** 074518

[22] Billah M M, Chowdhury M D H, Mativenga M, Um J G, Mruthyunjaya R K and Heiler G N 2016 *IEEE Electron. Dev. Lett.* **37** 735

[23] Kamiya T, Nomura K and and Hosono H 2009 *Phys. Status Solidi A* **206** 860

[24] Kamiya T, Nomura K, Hirano M and Hosono H 2008 *Phys. Status Solidi C* **5** 3098

[25] Ryu B, Noh H K, Choi E A and Chang K J 2010 *Appl. Phys. Lett.* **97** 022108

[26] Ji K H, Kim J I, Jung H Y, Park S Y, Choi R, Mo Y G and Jeong J K 2011 *Microelectronic Engineering* **88** 1412

[27] Kim J H, Kim U K, Chung Y J, Ji S J, *et al.* 2011 *Appl. Phys. Lett.* **98** 488

[28] Kim Y, Kim S, Kim W, Bae M, Jeong H K, Kong D, Choi S, Kim D M and Kim D H 2012 *IEEE Trans. Electron. Dev.* **59** 2699

[29] Nomura K, Kamiya T and Hosono H 2011 *Appl. Phys. Lett.* **99** 053505

[30] McWhorter P J and Winokur P S 1986 *Appl. Phys. Lett.* **48** 133

[31] Kouvatsos D N, Davidovic V, Papaioannou G J, Stojadinovic N, Michalas L, Exarchos M, Voutsas A T and Goustoridis D 2004 *Microelectronics Reliability* **44** 1631

[32] Loannidis E G, Tsormpatzoglou A and Tassos D H 2010 *J. Appl. Phys.* **108** 106103

[33] Chen W T, Lo S Y, Kao S C, Zan H W, Tsai C C, Lin J H, Fang C H and Lee C C 2011 *IEEE Electron. Dev. Lett.* **32** 1552

[34] Liu Y, Wu W J, Qiang Lei, Wang L, En Y F and Li B 2015 *Chin. Phys. Lett.* **32** 088506

[35] Hung K K, Ko P K, Hu C and Cheng Y C 1990 *IEEE Trans. Electron. Dev.* **37** 654

[36] Liu Y, Wu W J, Li B, En Y F, Wang L and Liu Y R 2014 *Acta Phys. Sin.* **63** 098503 (in Chinese)

[37] Ioannidis E G, Tsormpatzoglou A, Tassis D H, Dimitriadis C A, Templier F and Kamarinos G 2010 *J. Appl. Phys.* **108** 106103

[38] Tsormpatzoglou A, As N, Mahmoudabadi F, Choi N, Hatalis M K and Dimitriadis C A 2013 *IEEE Electron. Dev. Lett.* **34** 1403

[39] Liu Y, Chen H B, Liu Y R, Wang X, En Y F, Li B and Lu Y D 2015 *Chin. Phys. B* **24** 088503